Proceedings of the Korean Nuclear Society Spring Meeting
Kwangju, Korea, May 2002

Neutron Total and Capture Cross Sections on Mo-95, Tc-99, Ru-101 and Rh-103

Y. D. Lee and J. H. Chang

Korea Atomic Energy Research Institute
P.O. Box105, Yusung, Taejon, Korea 305-600

Abstract

The neutron induced nuclear data for Mo-95, Tc-99, Ru-101 and Rh-103 was calculated and evaluated from 10 keV to 20 MeV. The energy dependent optical model potential parameters were extracted based on the recent experimental data. Spherical optical model, statistical model in equilibrium energy, multistep direct and multistep compound model in pre-equilibrium energy and direct capture model were introduced in Empire calculation. The calculated results were compared with the evaluated files. The model calculated total and capture cross sections were in good agreement with the reference experimental data. The evaluated cross sections were compiled to ENDF-6 format and will improve the ENDF/B-VI.

1. Introduction

The evaluation for the selected fission products[1] has been jointly performed with National Nuclear Data Center (NNDC) of Brookhaven National Laboratory (BNL). The neutron cross section evaluation for Mo-95, Tc-99, Ru-101 and Rh-103 took place based on the experimental data from upper resonance region to 20 MeV. The current results will complement the resonance part to make full neutron data set.

Neutron induced nuclear reaction data for fission products are important for several applications: prediction of burnup performance in a fission reactor, criticality calculation for spent fuel storage design. Neutron capture cross sections of the selected fission product isotopes in several keV regions are important in a fission reactor concerning neutron absorption loss.

Mo-95, Ru-101 and Rh-103 are stable isotopes and Tc-99 has very long half life.

They are mainly accumulated from beta decay and electron capture from precursors in a reactor. Tc-99 is a material used in a super conducting material. Therefore, improved neutron data is required. In ENDF/B-VI, the evaluation on Mo-95 and Ru-101 has taken place at 1980 and 1992, for Tc-99 and Rh-103 at 1978. In the current evaluation, a proper model theory was applied based on the experimental data.

The evaluation consists of an optical model potential search followed by a complete nuclear reaction model calculation and validation to the experimental data. Nuclear reaction cross sections were calculated by using the recently released Empire-II code[2]. This code consists of several modules: optical model, Hauser-Feshbach model in equilibrium calculation, quantumn mechanical approach in pre-equilibrium and direct capture model. The width fluctuation correction in Hauser-Feshbach was calculated for the capture and inelastic scattering cross sections. The code offers several built-in libraries including the ENSDF nuclear level and decay schemes, nuclear masses, ground state deformations and γ-ray strength functions. The calculated cross sections are graphically compared with the experimental data and the evaluated files (ENDF/B-VI, JENDL-3.2, JEF-2.2, BROND-2 and CENDL-2). The evaluated results are compiled to ENDF-6 format.

2. Models

2.1 Optical Model Potential

For the isotopes, the potential in RIPL[3] does not reproduce the total cross section properly to the recent experimental data. Therefore, the proper potential form and corresponding parameters, as a function of incident neutron energy, were necessary to be searched in an optical model[4] based on the reference experimental data[5,6,7]. To obtain proper potential parameters, the Woods-Saxon well is used for the real part potential in optical model:

$$V(r) = -V/(1+\exp((r-R_v)/a_v)) \quad (1)$$

where V, a_v are the strength and diffuseness of the potential. The nuclear radius R_v, related to mass number A, is given by

$$R_v = r_v A^{1/3}. \quad (2)$$

For the imaginary part potential, the derivative Woods-Saxon shape is used,

$$W(r) = -4W\exp((r-R_w)/a_w) / 1+ \exp((r-R_w)/a_w)^2 \quad (3)$$

where W, R_w, a_w are potential strength, radius and diffuseness, respectively.

The real and imaginary potential strength and radius are expanded as a function of

incident neutron energy:

$$V = V_o + V_1 E_n, \quad r_v = r_o + r_1 E_n, \tag{4a}$$

$$W = W_o + W_1 E_n, \quad r_w = r_{wo} + r_{w1} E_n, \tag{4b}$$

where E_n is an incident neutron energy. The potential parameters in JENDL[8] were used as an initial value for the parameter searching process. s-wave strength function produced by JENDL potential was not satisfied to the reference value[9] evaluated in the resonance region. Potential parameters (V_o, V_1, W_o, W_1, r_o, r_1, r_{wo}, r_{w1}, a_v, a_w), including parameters for spin-orbit coupling: V_{so}, r_{so}, a_{so}, were searched from 1 keV to 20 MeV. The potential parameters produce total, elastic scattering and reaction cross sections, s- and p-wave strength function values and transmission coefficients.

2.2 Capture

Empire-II was used to compute each reaction cross sections using the transmission coefficients obtained from the optical model. Empire accounts for the major nuclear reaction mechanisms, such as Multistep Direct (MSD), Multistep Compound (MSC) and the full featured Hauser-Feshbach model. The MSD takes care of the inelastic scattering to vibrational collective levels and decay information. The MSD theory of pre-equilibrium scattering to the continuum is based on Tamura, Udagawa and Lenske[10]. In MSC approach, the modeling follows the approach of Nishioka et at. (NVWY)[11].

3. Evaluation

The searched potential parameters are summarized in Table I. The potential depth for real part was not changed significantly in the isotopes. The potential for spin-orbit coupling did not give much influence on neutron cross section data. s-wave strength function (S_o) was calculated at 1 keV in the optical model, by the searched potential parameters. In Table II, the calculated S_o values are close to those by the recently evaluated resonance parameters in the unresolved resonance energy region.

All input parameters for Empire were tuned to fit the capture calculation to the experimental data. The calculated cross sections were graphically compared with the experimental data and evaluated files. Fig. 1 shows the comparison of the calculated result to the experimental data[5] and ENDF/B-VI for total cross section of Mo-95. The model calculated total cross section by the searched optical model potential was in good agreement with the experimental data. ENDF/B-VI shows the difference from the

calculation and experimental data in the whole energy region. Fig. 2 shows the (n, γ) cross section results. The calculation follows the experimental data[12] very well and shows the direct capture contribution of around 14 MeV. There is good agreement with ENDF/B-VI until 3 MeV.

Fig. 3 shows the calculated total cross section with the experimental data[6] and the evaluated files for Tc-99. The model calculation follows well the reference experimental data in the high energy region. At low energy, s-wave strength function value was referenced from the evaluation of resonance parameters[9]. Fig. 4 shows the capture cross section. In the measurement energy range, the calculation is in good agreement with the experimental data[13,14]. Between 200 keV and 1 MeV, the calculation shows the difference from the ENDF/B-VI.

The total cross section for Ru-101 was calculated and compared with the evaluated files in Fig. 5. There is no experimental data. Therefore, s-wave strength function value from the evaluation of resonance parameters[9] was referenced to generate the total cross section. Fig. 6 shows the capture cross section. The calculated capture cross section is in good agreement with the reference experimental data[15]. ENDF/B-VI is lower than the calculation and experimental data in the measured energy range.

Fig. 7 shows the total cross section of Rh-103. The calculation is in good agreement with the measured data[7]. The calculation is pretty close to ENDF/B-VI in whole region. Fig. 8 is the capture cross section. Model calculation shows good agreement with the measured data [7] and ENDF/B-VI. The elastic scattering and other threshold reaction cross sections are not shown here, but the results will be summarized and published later[16].

4. Conclusion

The searched energy dependent optical model potential was proper to produce the calculated total and capture cross sections in the evaluation energy range. The s-wave strength function was helpful in obtaining the total cross section closer to the experimental data, moreover, when there was no experimental data. Empire was successful in producing and enhancing the capture cross section. The results will be submitted in the ENDF/B-VI to improve neutron data.

Acknowledgements

This work is performed under the auspices of Korea Ministry of Science and

Technology as a long-term R&D project.

References

[1] J.H. Chang et al., Establishment of Nucelar Data System, KAERI/RR-2121/2000.
[2] M. Herman, Empire-2: Statistical Model Code for Nuclear Reaction Calculations, IAEA, 2000.
[3] S. Igarasi, Optical Model Potentials used in JENDL Evaluations (JAERI, Tokai-mura, Japan), Reference Input Parameter Library for theoretical calculations of nuclear reactions (RIPL), JAERI 1228(41), 1973.
[4] R.D. Lawson, ABAREX_A Neutron Spherical Optical-Statistical Model Code, in Workshop on Computation and Analysis of Nuclear Data Relevant to Nuclear Energy and Safety, pp447, Trieste, Italy.
[5] M.V. Pasechnik et al., “Total Neutron Cross Sections for Molybdenum and Zyrconium at Low Energies,” C, 80KIEV, 1, 304, 1980.
[6] D.G.Foster JR, D.W. Glasgon, “Neutron Total Cross Sections, 2.5 - 15 MeV,” J, PR/C, 3, 576, 1971.
[7] M.V. Bokhovko et al., “Neutron Radiation Cross-Section, Neutron Transmission And Average Resonance Parameters For Some Fission Product Nuclei,” R, FEI-2168-91, 1991.
[8] T. Nakagawa, et al., Japanese Evaluated Nuclear Data Library, Version 3, Revision 2, J. Nucl. Sci. Technol. 32, 1259, 1995.
[9] S.Y. Oh and J.H.Chang, Neutron Cross Section Evaluations of Fission Products below the Fast Energy Region, BNL-NCS-67469 (KAERI/TR-1511/2000), Brookhaven Natoinal Laboratory.
[10] T. Tamura, T. Udagawa and H. Lenske, Phys. Rev. C26, 379, 1982.
[11] H. Nishiok, J.J.M. Verbaarschot, H.A. Weidenmuller and S. Yoshida, Ann. Phys. 172, 67, 1986.
[12] A.R.DEL.Musgrove et al., “Average Neutron Resonance Parameters and Radiative Capture Cross Sections for the Isotopes of Molybdenum,” J, NP/A, 270, 108, 1976.
[13] R.L. Macklin, “Technetium-99 Neutron Capture Cross Section,” J, NSE, 81, 520, 1982.
[14] S.M. Qaim, “Nuclear Reaction Cross-Sections for 14.7 MeV Neutrons on TC-99,” J, JIN, 35, 3669, 1973.
[15] R. W. Hockenbury, "Capture Cross sections of 145-Nd, 149-Sm, 101-Ru, 102-Ru, and 104-Ru," Bull. Amer. Phys. Soc., Vol.20, pp560, 1975.
[16] Y.D. Lee and J.H. Chang, “Neutron Cross Section Evaluation on Mo-95, Tc-99, Ru-101 and Rh-103 in the Fast Energy Region,” to be published at J. of KNS, 2002.

Table I: Potential parameters as a function of incident neutron energy

Parameter (unit)	Mo-95	Tc-99	Ru-101	Rh-103
V_o(MeV)	46.00	47.50	47.50	46.81
V_1(MeV)	-0.25	-0.30	0.00	-0.40
r_o(fm)	1.291	1.290	1.282	1.234
a_v(fm)	0.670	0.620	0.620	0.665
W_o(MeV)	7.000	9.740	9.740	7.906
r_{wo}(fm)	1.401	1.425	1.415	1.450
a_w(fm)	0.410	0.350	0.410	0.437
V_{so}(MeV)	7.000	7.000	7.000	7.033
r_{so}(fm)	1.291	1.290	1.282	1.241
a_{so}(fm)	0.620	0.620	0.620	0.500
W_1(MeV)	0.0000	0.1000	0.0000	-0.1138
r_{w1}(fm)	0.000	0.000	0.000	0.000
r_1(fm)	0.000	0.000	0.000	-0.010

Table II: Comparison of s-wave strength function

Isotopes	s-wave strength function	
	In optical model[4]	By evaluation[9]
Mo-95	0.51E-4	0.45E-4
Tc-99	0.43E-4	0.43E-4
Ru-101	0.62E-4	0.62E-4
Rh-103	0.53E-4	0.57E-4

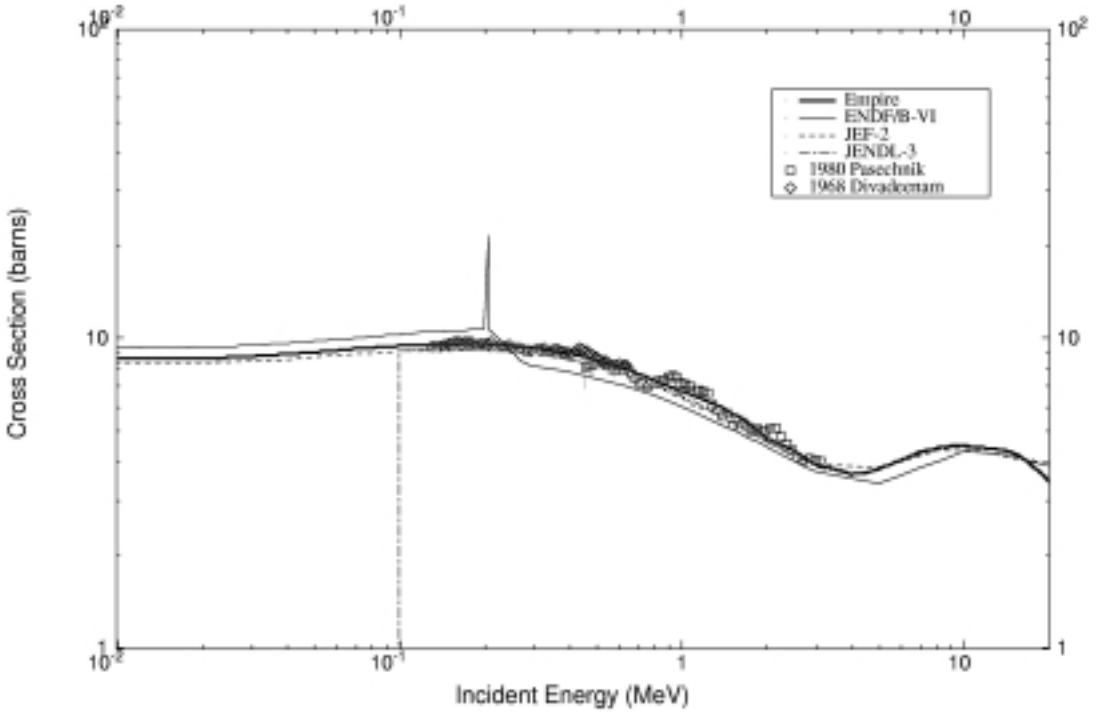

Fig. 1. Total cross section of Mo-95.

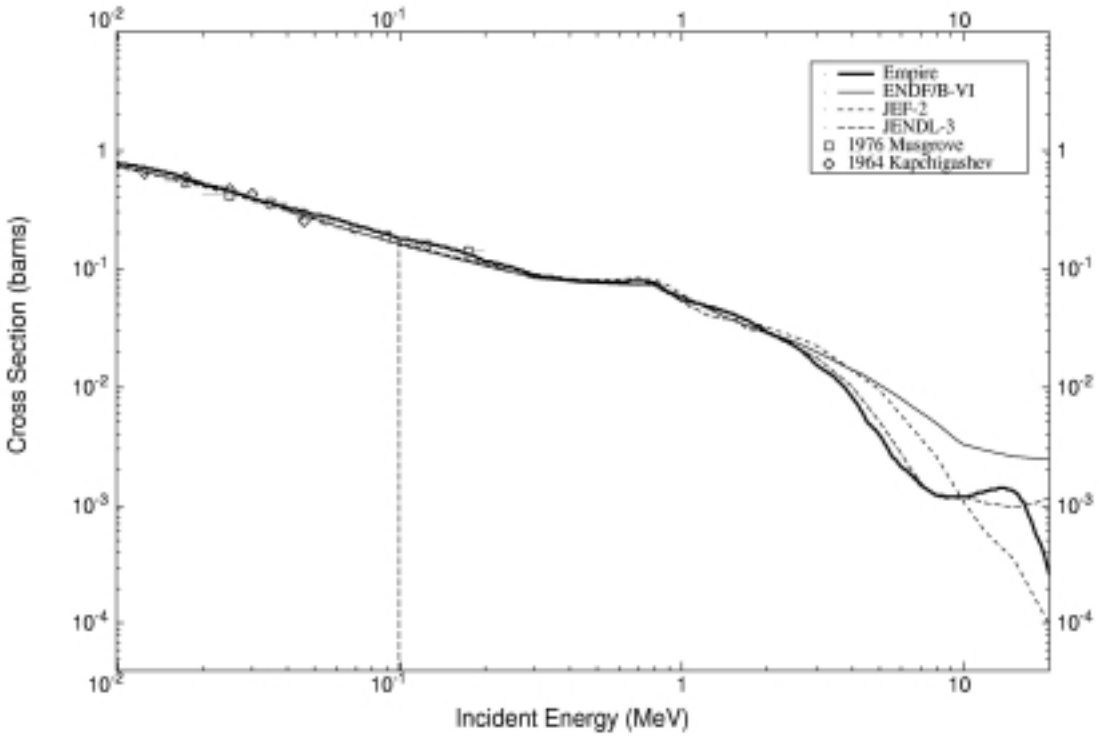

Fig. 2. (n, γ) cross section of Mo-95.

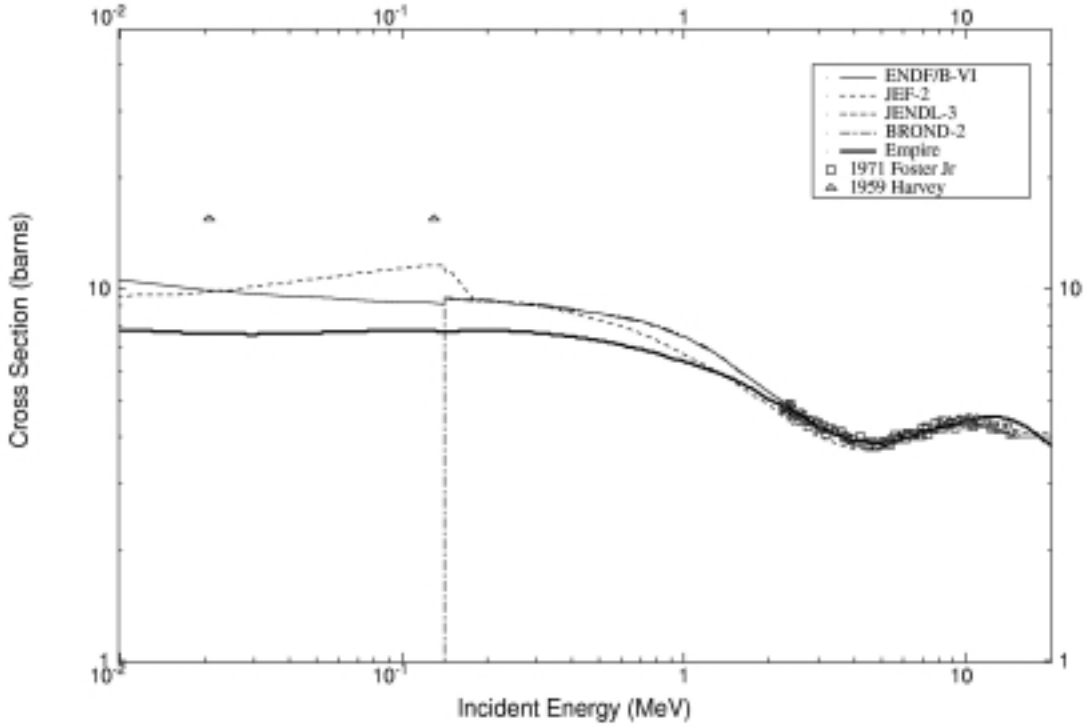

Fig. 3. Total cross section of Tc-99.

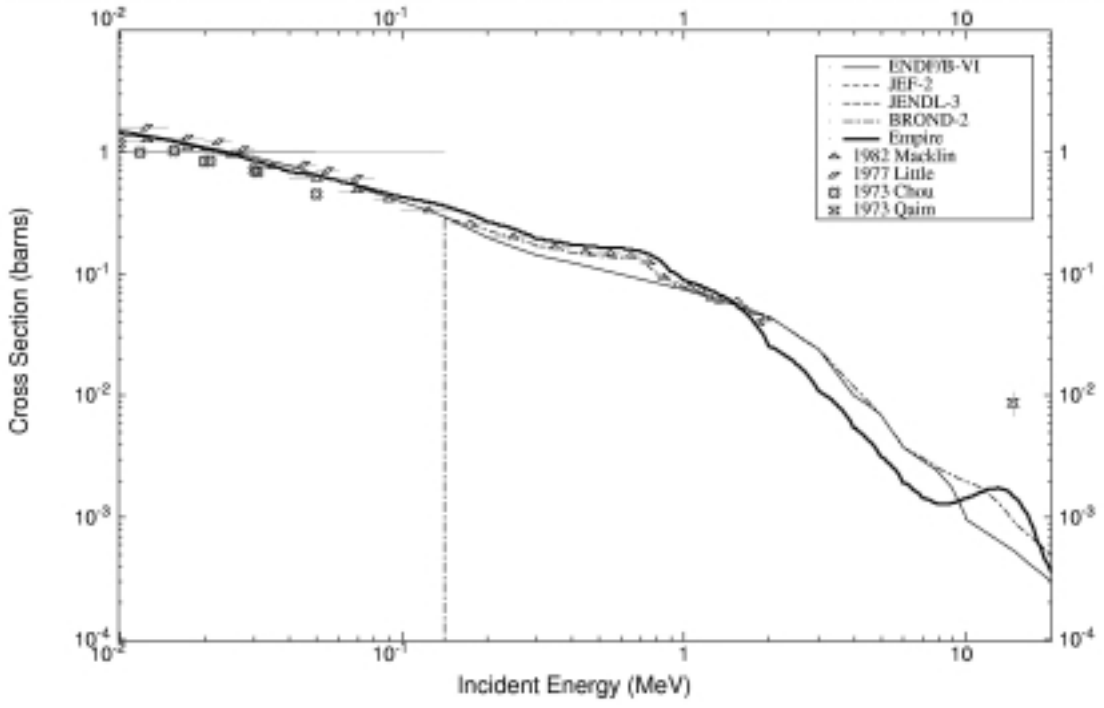

Fig. 4. (n, γ) cross section of Tc-99.

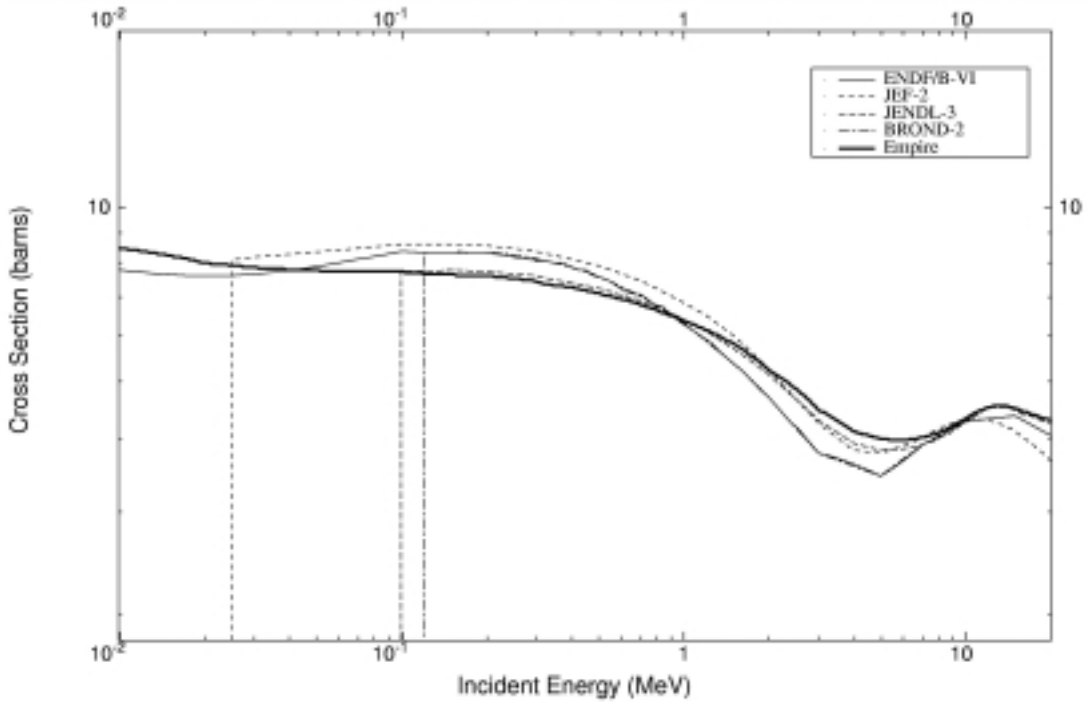

Fig. 5. Total cross section of Ru-101.

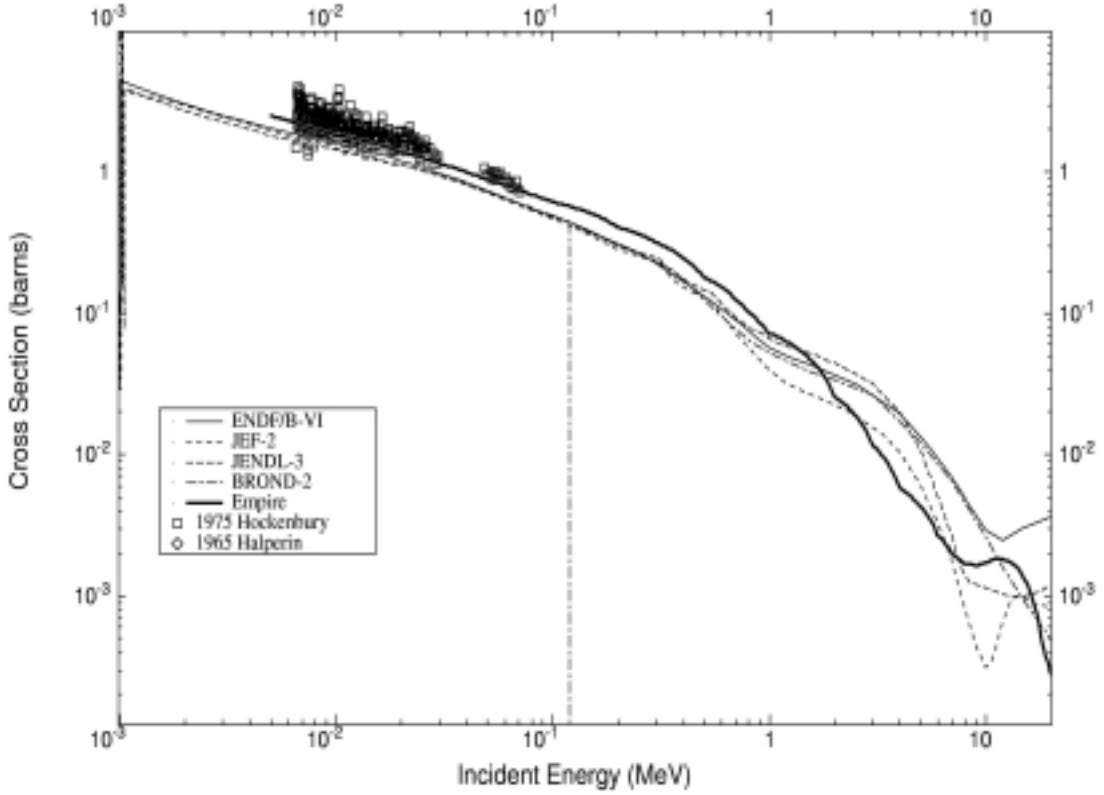

Fig. 6. (n, γ) cross section of Ru-101.

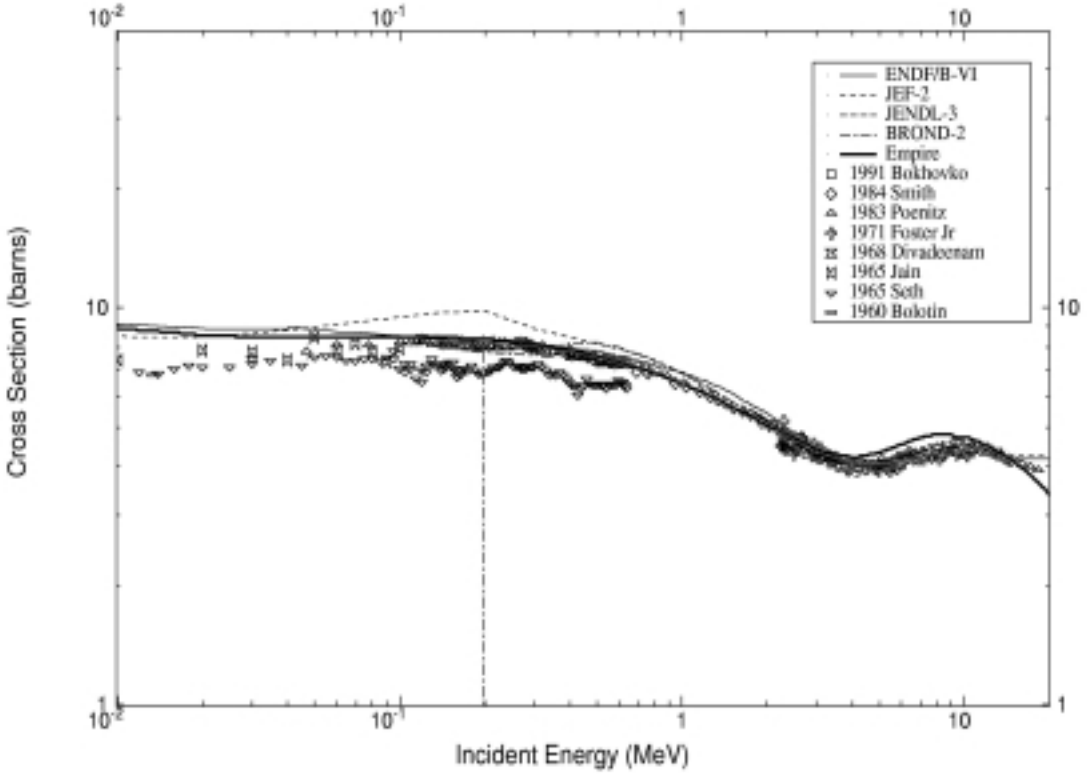

Fig. 7. Total cross section of Rh-103.

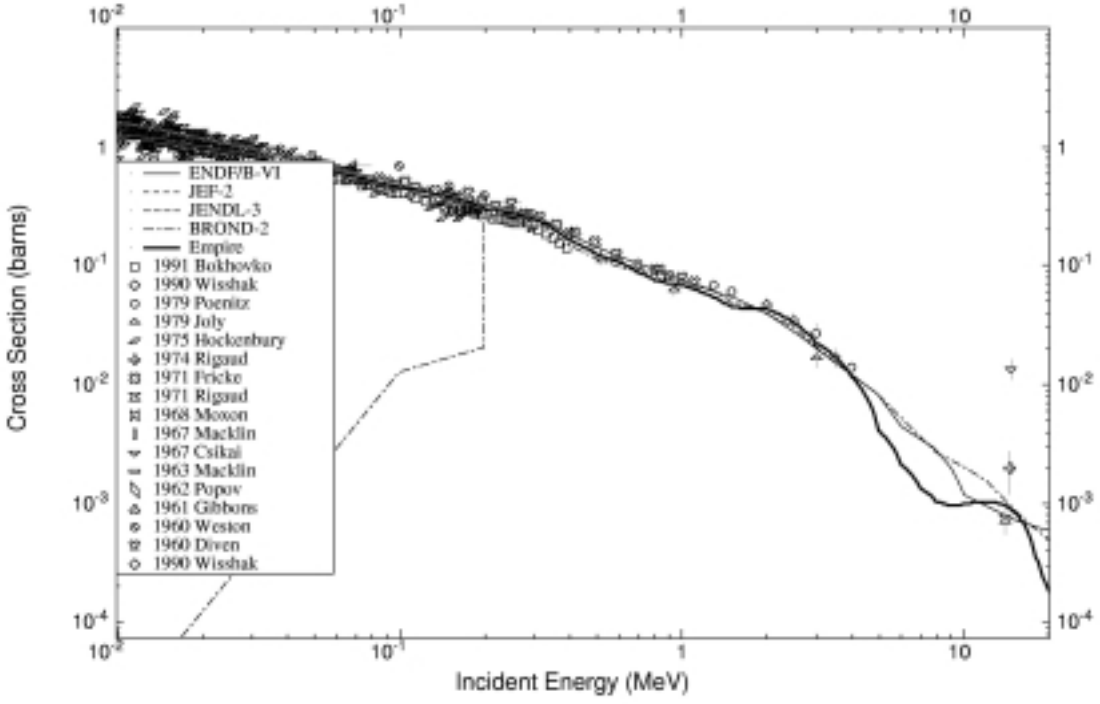

Fig. 8. (n, γ) cross section of Rh-103.